

**Isolation and Crystallographic Characterization of  $\text{La}_2\text{C}_2@\text{C}_s(574)\text{-C}_{102}$   
and  $\text{La}_2\text{C}_2@\text{C}_2(816)\text{-C}_{104}$ : Evidences for the Top-Down Formation  
Mechanism of Fullerenes**

Wenting Cai, Fang-Fang Li, Lipiao Bao, Yunpeng Xie, and Xing Lu\*

State Key Laboratory of Materials Processing and Die & Mold Technology,  
School of Materials Science and Engineering, Huazhong University of  
Science and Technology (HUST), Wuhan 430074 (China).

Email: lux@hust.edu.cn

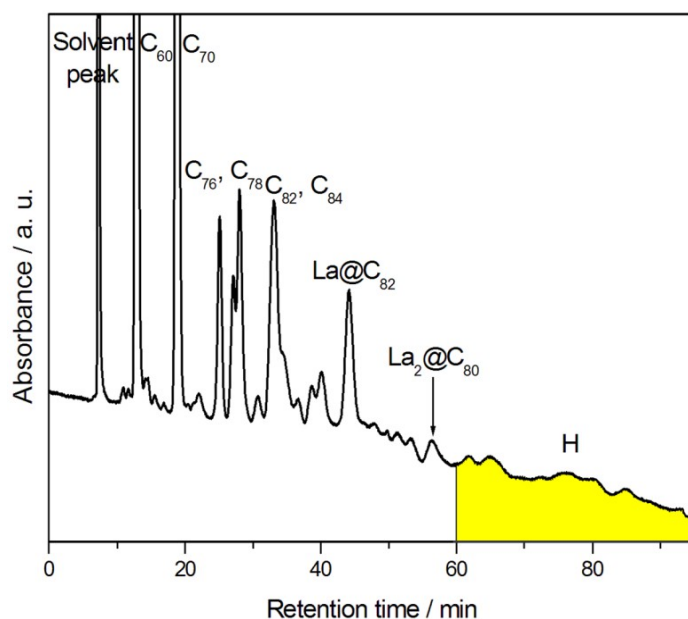
**Experimental details:**

**HPLC separation of  $\text{La}_2\text{C}_2@\text{C}_s(574)\text{-C}_{102}$  and  $\text{La}_2\text{C}_2@\text{C}_2(816)\text{-C}_{104}$ .** The first stage was performed on a 5PYE column (20 mm × 250 mm, Cosmosil Nacalai Tesque) with toluene as mobile phase. Figure S1 shows the first stage HPLC chromatogram. The fraction eluting after 60 minutes, named as H, was collected. Fraction H was then injected into a BPM column (20 mm × 250 mm, Cosmosil Nacalai Tesque) for the second stage separation using chlorobenzene as the eluent. The fraction marked with H1 shown in Figure S2 was collected. The third stage was carried out using a 5PBB column (20 mm × 250 mm, Cosmosil Nacalai Tesque) with a chlorobenzene mobile phase, as shown in Figure S3. Nine fractions, which were named as H1-1 to H1-9, were collected. After that, the last two fractions H1-8 and H1-9 were re-injected into a Buckyprep column (20 mm × 250 mm, Cosmosil Nacalai Tesque) for the fourth stage separation using chlorobenzene as the eluent, and  $\text{La}_2\text{C}_{104}$  and  $\text{La}_2\text{C}_{106}$  were finally obtained (Figures S4&S5). The purities of the isolated species were then reconfirmed by chromatography on a Buckyprep column (4.6 mm × 250mm, Cosmosil Nacalai Tesque) with chlorobenzene at a flow rate of 0.7 mL/min, along with the LDI-TOF mass spectrometry in a negatively charged mode (Figure 1a and 1b).

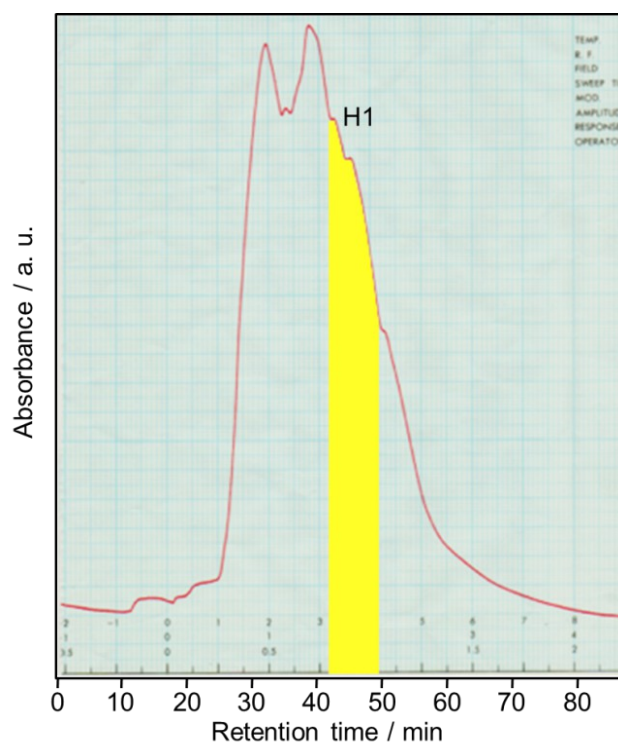
**Single-crystal X-ray results of  $\text{La}_2\text{C}_2@\text{C}_s(574)\text{-C}_{102}$ .** Eighteen La positions are found for the two La atoms and are arranged in the form of an umbrella shape with respect to the disordered positions of  $\text{C}_2$  unit. Eight of them, which positioned under the corannulene fraction of the cage passes through the longest axis of the cage, are perpendicular to the rest of ten sites beneath the opposite terminal of the cage (Figure S7). La1 and La1A, with fractional occupancies of 0.24 each, are the most prominent sites on opposite sides of

the C<sub>2</sub> unit, respectively. The specific occupancies of other La positions range from 0.14 to 0.03 as follow: La2, 0.11; La3, 0.07; La4, 0.11; La5, 0.11; La6, 0.10; La7, 0.16; La8, 0.07; La9, 0.02; La10, 0.01; La2A, 0.07; La3A, 0.16; La4A, 0.07; La5A, 0.14; La6A, 0.14; La7A, 0.10; La8A, 0.08. There are three disordered positions in the C<sub>2</sub> unit. C1 and C2 are the predominant positions with fractional occupancy of 0.40, while the other two pairs of C<sub>2</sub> unit have lower occupancies of 0.38 and 0.22, respectively (Table S1).

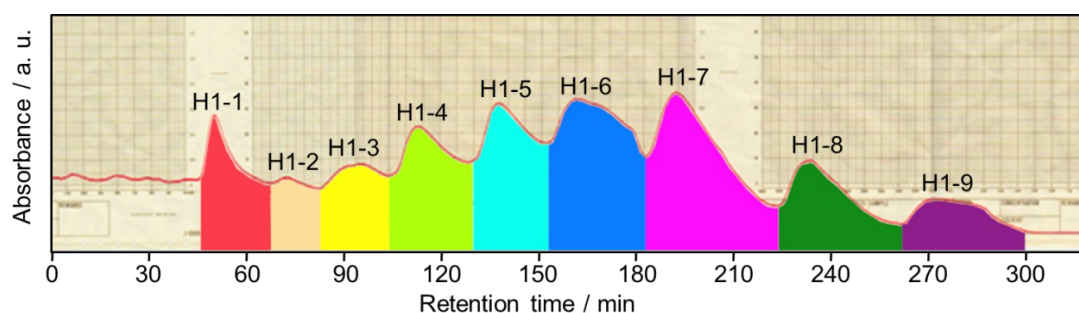
**Single-crystal X-ray results of La<sub>2</sub>C<sub>2</sub>@C<sub>2</sub>(816)-C<sub>104</sub>.** Six disordered positions are found for the two La atoms in C<sub>2</sub>(816)-C<sub>104</sub>. Two La sites are positioned on the left of the C<sub>2</sub>-unit with similar occupancy values (0.27 and 0.23), and the rest four La sites are located on the right of the C<sub>2</sub>-unit. La1A is the major site with an occupancy of 0.32, while La2A, La3A, La4A have occupancies of 0.13, 0.03, 0.02, respectively. In addition, the structure of La<sub>2</sub>C<sub>2</sub>@C<sub>2</sub>(816)-C<sub>104</sub> includes two disordered positions of the C<sub>2</sub>-unit. The C1-C2 distance of the major position (0.38 occupancy) is 0.93(3) Å, while the C3-C4 distance of the minor position (0.12 occupancy) is 0.90(6) Å (Table S2).



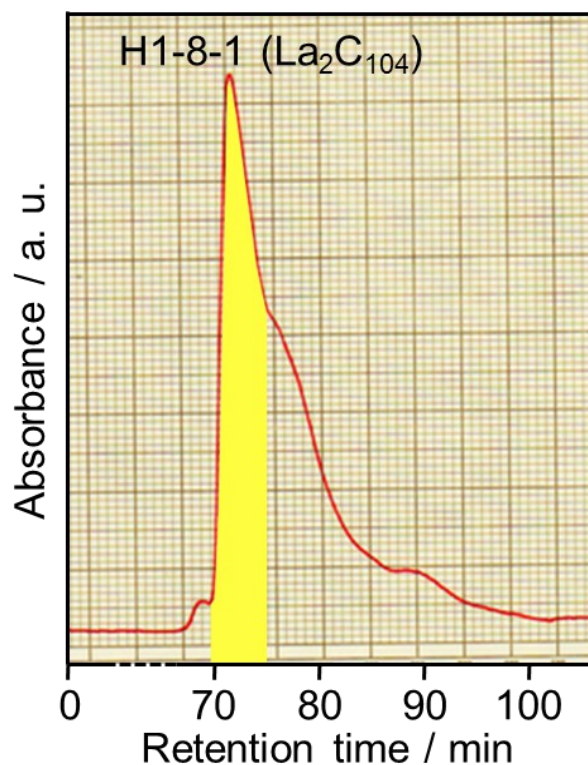
**Figure S1.** The first stage HPLC chromatogram of extract. HPLC conditions: 5PYE column,  $\phi = 20 \text{ mm} \times 250 \text{ mm}$ ; eluent = toluene; flow rate = 9.99 mL/min; detecting wavelength = 390 nm.



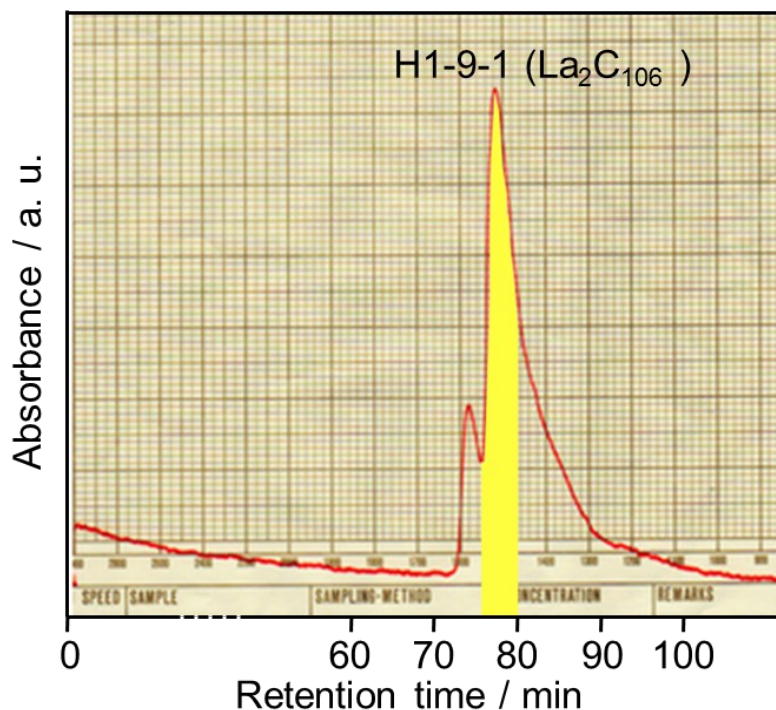
**Figure S2.** The second stage HPLC chromatogram of fraction H. HPLC conditions: BuckyPrep M column,  $\phi = 20 \text{ mm} \times 250 \text{ mm}$ ; eluent = chlorobenzene; flow rate = 8 mL/min; detecting wavelength = 390 nm.



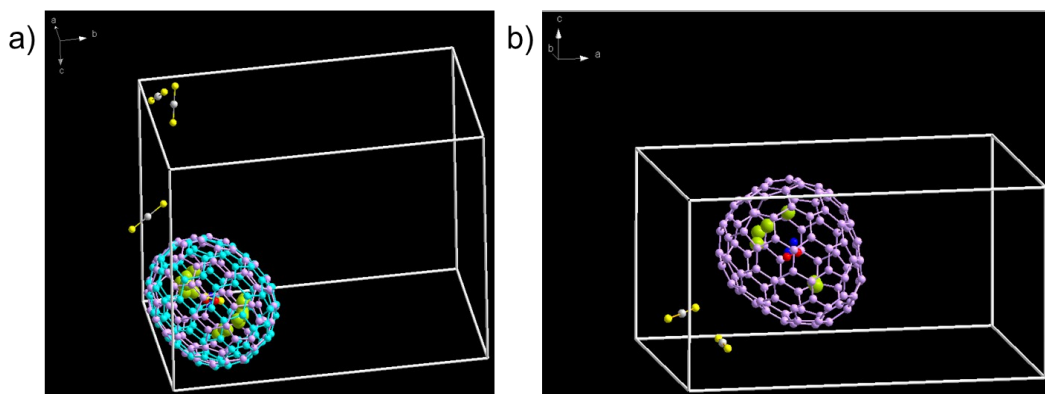
**Figure S3.** The third stage HPLC chromatogram of fraction H1. HPLC conditions: 5PBB column,  $\phi = 20 \text{ mm} \times 250 \text{ mm}$ ; eluent = chlorobenzene; flow rate = 8 mL/min; detecting wavelength = 390 nm.



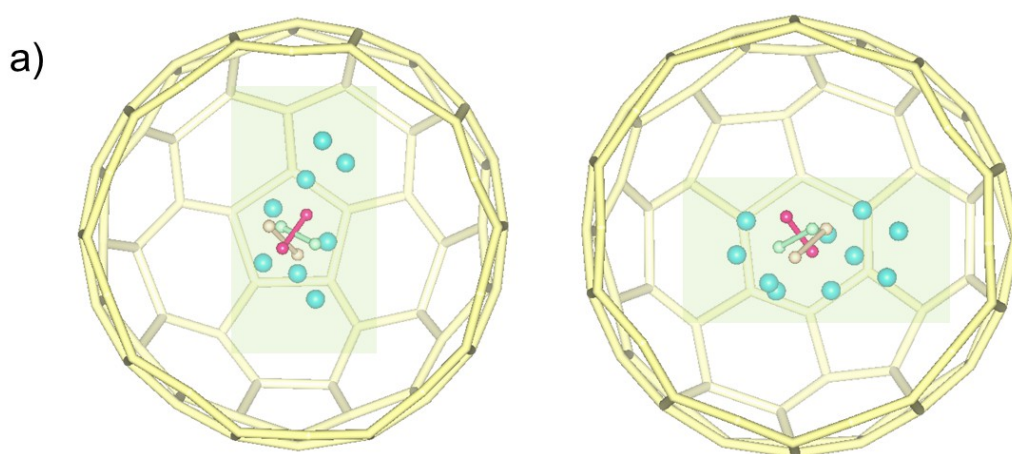
**Figure S4.** The fourth stage HPLC chromatogram of fraction H1-8. HPLC conditions: BuckyPrep column,  $\phi = 20 \text{ mm} \times 250 \text{ mm}$ ; eluent = chlorobenzene; flow rate = 3.5 mL/min; detecting wavelength = 390 nm.



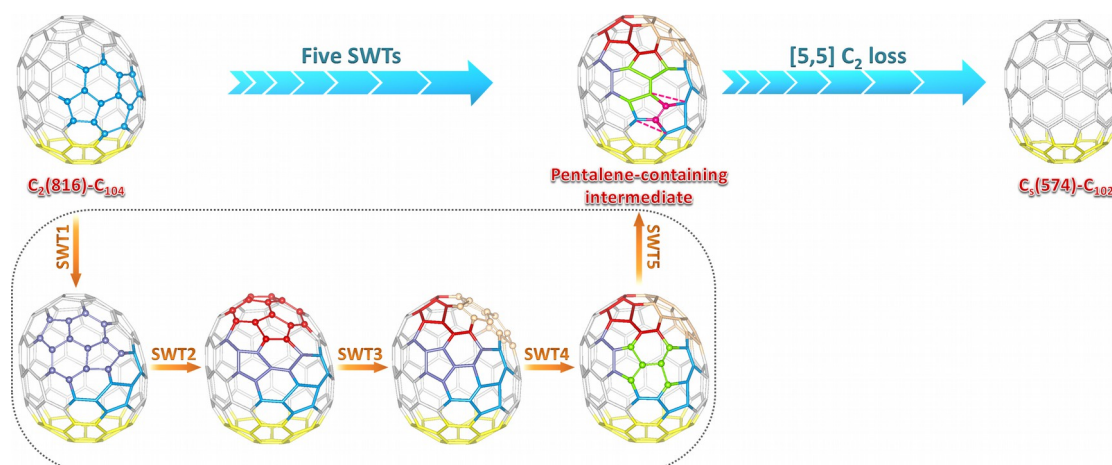
**Figure S5.** The fourth stage HPLC chromatogram of fraction H1-9. HPLC conditions: BuckyPrep column,  $\phi = 20 \text{ mm} \times 250 \text{ mm}$ ; eluent = chlorobenzene; flow rate = 3.5 mL/min; detecting wavelength = 390 nm.



**Figure S6.** (a) A view of  $\text{La}_2\text{C}_2@\text{C}_s(574)\text{-C}_{102}\cdot 3(\text{CS}_2)$  in the asymmetric crystal unit. (b) A view of  $\text{La}_2\text{C}_2@\text{C}_2(816)\text{-C}_{104}\cdot 3(\text{CS}_2)$  in the asymmetric crystal unit.

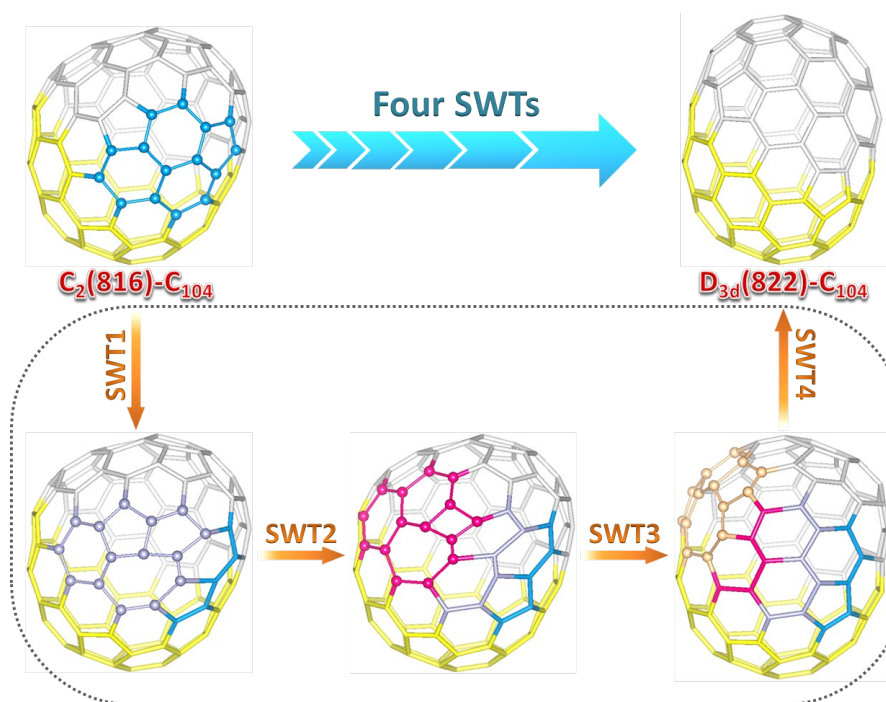


**Figure S7.** The distribution of La positions for one La atom under the corannulene fraction of the cage (left) and the distribution of La positions for the other La atom beneath the opposite terminal of the cage (right), as viewed down the longest axis of the major  $\text{C}_{102}$  cage, respectively.

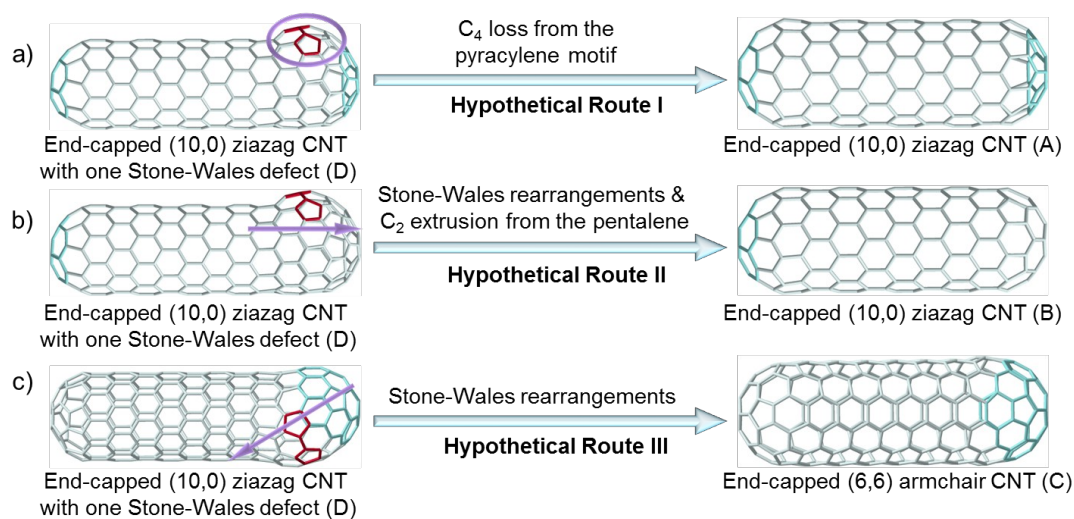


**Figure S8.** Structural rearrangements from  $\text{C}_2(816)\text{-C}_{104}$  to  $\text{C}_s(574)\text{-C}_{102}$ . Each step is highlighted with different colored atoms. Note that the corannulene fragment, which is consistent with that of  $\text{C}_s(574)\text{-C}_{102}$ , is shown in yellow.





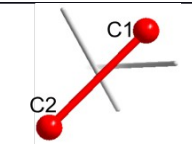
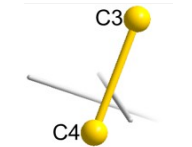
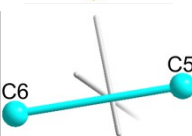
**Figure S9.** Structural rearrangements from  $C_2(816)-C_{104}$  to  $D_{3d}(822)-C_{104}$  via four Stone-Wales transformation steps. Each step is highlighted with different colored atoms. Note that the partial region, which is consistent with that of  $D_{3d}(822)-C_{104}$ , is shown in yellow.



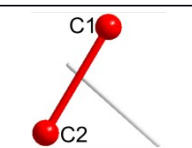
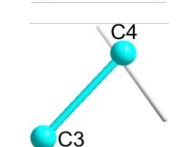
**Figure S10.** The formation mechanisms of ideal CNTs from a defective CNT revealed at the atomic level. The arrows in b and c denote the growth direction of the new tube. Multiple color codes are used to enhance visualization.

**Table S1.** The C-C distances and the corresponding fractional occupancies of the three disordered positions of the  $C_2$ -unit in  $La_2C_2@C_3(574)-C_{102}$ .

Labeling	Orientation	C-C bond length (Å)	Fractional occupancy
----------	-------------	---------------------	----------------------

C1-C2		1.05(4)	0.40
C3-C4		0.91(5)	0.38
C5-C6		1.28(5)	0.22

**Table S2.** The C-C distances and the corresponding fractional occupancies of the two disordered positions of the C<sub>2</sub>-unit in La<sub>2</sub>C<sub>2</sub>@C<sub>2</sub>(816)-C<sub>104</sub>.

Labeling	Orientation	C-C bond length (Å)	Fractional occupancy
C1-C2		0.93(3)	0.38
C3-C4		0.90(6)	0.12